Available online at www.pelagiaresearchlibrary.com

Pelagia Research Library

Advances in Applied Science Research, 2015, 6(8):17-35

ISSN: 0976-8610
CODEN (USA): AASRFC

Fractured basement reservoir identification using geophysical well log data, Gulf of Suez, Egypt

Mohamed S. El Sharawy

Geophysical Sciences Department, Room 405, Physics Building, El Behouth St., National Research Centre, Dokki, Cairo, Egypt

ABSTRACT

Naturally fractured reservoirs produced hydrocarbon from several localities throughout the world. The fractured reservoirs can be fractured sandstone, fractured carbonate or fractured basement. In this concern, four types of fractured reservoirs were identified according to the contribution of fractures. The fractured basement reservoir is the one, in which fractures provide the essential porosity and permeability. In the southern Gulf of Suez, Egypt, several oil fields have been produced hydrocarbon from fractured basement, such as Zeit Bay, Hilal, Ashrafi and Shoab Ali. In this study, we used conventional geophysical well logs, routine core analysis and 2D seismic data to identify the fractured basement in some bore holes distributed throughout the southern Gulf of Suez, Egypt. The results indicate that the productive wells from fractured basement usually overlain by a hydrocarbon column from which they are sourced. The results show also that all the studied wells contain fractured rocks at the top of the basement interval with varying of thickness from one well to another. It can be concluded also that the well logs are powerful tools to identify the fractured basement especially resistivity and FIL logs.

Keywords: basement, fractures, Gulf of Suez, well logs

INTRODUCTION

Fracture reservoirs are common in petroleum exploration and production despite their difficulties in detection and evaluation for geologist, geophysicists and engineers. The term “fracture” referred to any series of discontinuous features in rocks such as joints, faults, fissures and/or bedding planes. The fractured lithology could be sandstone, carbonates or basement. According to Nelson [1], naturally fractured reservoirs can be classified into four types. Type 1: fractures provide essential porosity and permeability. Type 2: fractures provide essential permeability. Type 3: fractures provide assistance permeability in an already producible reservoir. Type 4: fractures provide neither additional porosity nor permeability but create significant reservoir anisotropy. The fractured basement reservoirs are corresponding to reservoir type C, as classified by Aguilera [2]. He stated that this type of reservoir started with high production rate declined in a short period to uneconomic rate. Luthi [3] stated that the most difficult problem associated with fractured basement reservoir is to evaluate their capacity and reserve. In this concern, several contributions were introduced to evaluate the fractured basement reservoir characterizations [4-9].

In this study, Landes et al. [10] definition of basement is adopted, in which basement rocks are considered as any metamorphic or igneous rocks in spite of age unconfromably overlain by sedimentary sequence. Associated uplift or structural highs are common in basement reservoir; as a consequence, basement rocks have suffered from a long period of weathering and erosion. Such weathering and erosion, provide the way to create porosity and permeability, in which hydrocarbon can be accumulated and sourced from the permeable rocks. Basement reservoirs are documented in several countries such as Algeria, china, Vietnam, Canada, India, Yemen and Egypt [5-6].

In 1981, Zeit Bay field, Gulf of Suez, Egypt, was discovered by drilling QQ 89-1 well in the western margin of the southern Gulf of Suez with a new reservoir discovery (basement). Since then, pre – Cambrian basement rocks have been considered as a tertiary reservoir in the Gulf of Suez Province. The production started in this field with about 20000 BOPD reached apex in the mid 80's with about 80000 BOPD and declined to about 50000 BOPD in 2011 [11]. It must be noted that this rate of production comes from a long hydrocarbon column extended from Hammam Faraun Member of the Belayim Formation (Middle Miocene) to the pre – Cambrian basement. According to Zahran and Askary [12], the flow rates per well for fractured basement vary from 7000 to 9000 BOPD. The fractured basement of the Zeit Bay field has been captured the attention of the researchers, in which numerous studies focused on this field [12-14]. However, several other fields in the southern Gulf of Suez were documented to produce hydrocarbon from basement, such as Ashrafi, Hilal, Shoab Ali Geisum [15]. The Gulf of Suez basement rocks are highly heterogonous usually capped by high density brecciated zone and consists mainly of metavolcanic, granitic and metasediments. In this study, we used the available well logs, 2D seismic data as well as the routine core analysis results to identify and evaluate the basement reservoirs in the southern Gulf of Suez.

2. Data and methods:

Eight bore holes distributed throughout the southern Gulf of Suez, Egypt, were selected. These wells are SB374-2C (374 field), SDK7 (Sidki field), GS392-2, Hil -A3B and Hil –A9A (Hilal field), AS404-C1X (Ashrafi field) and GH395-1 and D3 (Shoab Ali field). These wells belong to two different structural trends; B –Trend in the central trough of the Gulf of Suez and Ghara Trend toward the eastern margin of the Gulf of Suez (Fig. 1). Both trends represented structure highs. The available data are gamma ray, natural spectral gamma ray (for SDK-7& AS40-C1X wells), resistivity (induction medium and deep; laterolog shallow, deep and microspherical focused log), sonic, density, neutron, Pe curve, dipmeter (cluster processing and FIL processing), repeat formation tester (RFT) and variable density log (VDL for Hil –A3B). Beside geophysical logs, some 2-D seismic lines are available. Routine core analysis was available for SDK -7, Hil –A9A, Hil – A3B, and AS 404-C1X wells. These core analyses include description for the rocks and determination of porosity, permeability, fluid saturation and grain density.

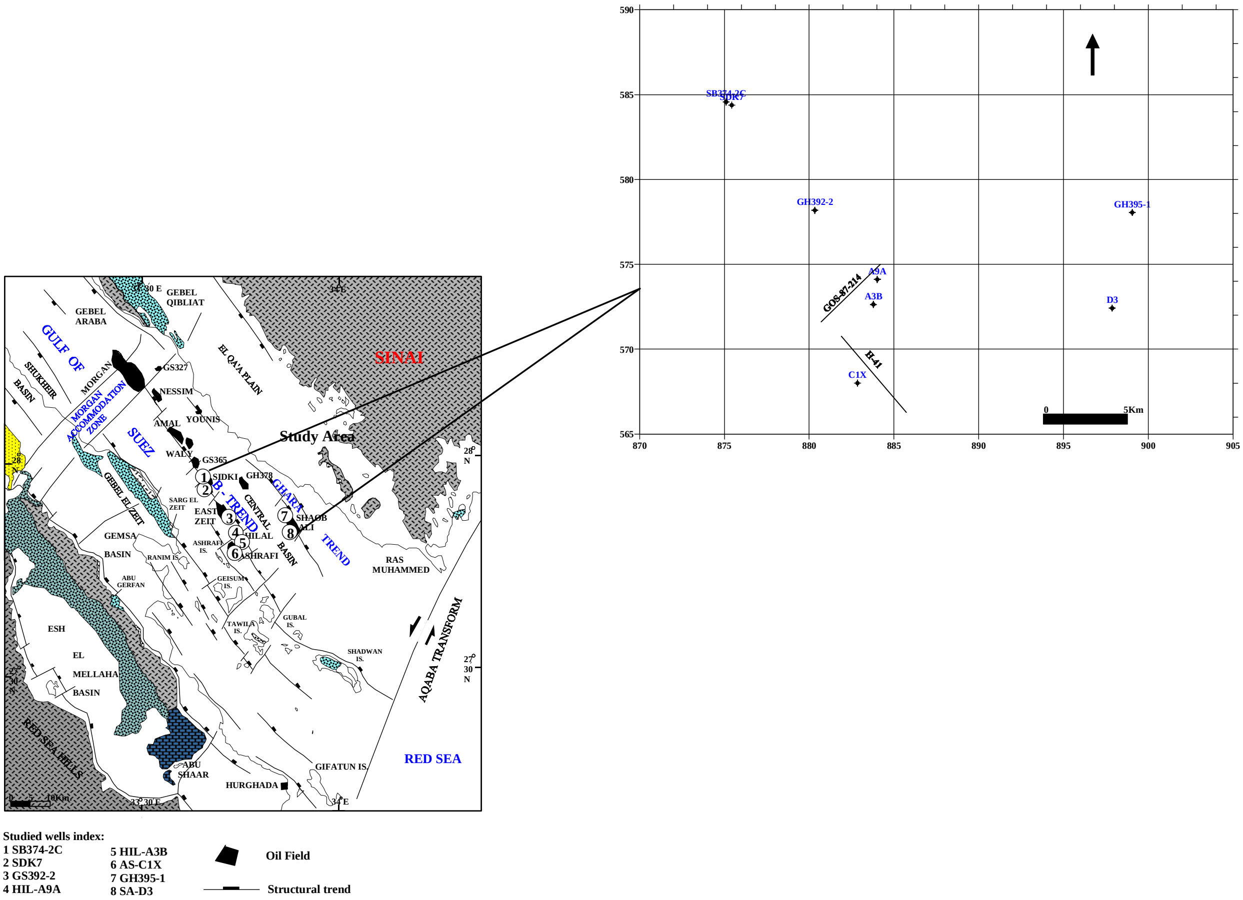

Fig. (1): Location map of the study area showing the main structural trends and oil fields, studied wells distribution and the used seismic lines

In Hil –A3B well, the basement rock consists of rosy, dark pink, cracked, sharp edged hard feldspars (orthoclase), with up to 10% dark grey, occasionally light grey, quartz grains, with trace of strained mafic occasionally black mafic minerals, with no oil staining. Downward, the percentage of feldspars decreased to 60% with very coarse crystals of dark pink, rosy, hard – very hard cracked, sharp edged feldspars (orthoclase), with 20% dark green, pearly luster 10% light grey to dark grey, gravel size very coarse grained of quartz, with 10% dark black mafic minerals, with no oil shows. Further downward, the basement rock composed of 50% dark black, pearly luster, soapy feeling, glassy, very hard, mafic minerals, possibly chlorite, 20% pink rosy occasionally reddish brown, very hard, sharp edged feldspars (or thoclase) with 10% light dark grey coarse grained hard quartz grains.

In AS40-C1X from 1844.6 -1848.4 m depth, the basement rock consists of fractured granite with– light brown, buff, pink, orange; white consisted of orthoclase, feldspars, quartz, with clear crystalline mafic mineral of biotite, mica, muscovite, holocryst in part, fractured. At 1848.4-1849 m depth, altered granite is fractured, white gray, green, occasionally brown, orange, buff, mainly quartz and secondary chlorite, with oil smell, stain, with very good golden yellow direct floresence. Between 1849-1852 m depth, granite is reddish brown to grayish white. Quartz is white to translucent, coarse to medium grains Orthoclase is pink, orange, coarse crystalline, also containing biotite, mica, muscovite and mafic minerals. Notes, the core has a rare fracture allover the 3 meters with hydrocarbon smell in fracture, with good golden yellow direct fluorescence, with good yellow crush cut fluorescence. Between 1866-1867.8 m depth, granite is reddish brown to grayish white. Quartz is white to translucent, coarse to medium grains Orthoclase is pink, orange, coarse crystalline, also containing biotite, mica, muscovite and mafic minerals. Notes, the core has some fracture mainly vertical more than core interval from 1849-1852 m depth. Shows indicate oil smell in fracture, with good golden yellow direct fluorescence, with good yellow crush cut fluorescence. Between 1970- 1970.5 m depth, granite description as in the above interval (1866-1867.8 m depth) with hydrocarbon smell in fractures, with poor to very poor fluorescence.

In SDK – 7 well, the cored interval is about 58 ft thick revealed that both vertical and horizontal permeability are less than 0.01 md except for two samples (0.37 & 0.77 md). Helium porosity ranged from 0.002 to 0.143 with an average value of 0.023. The grain density ranged from 2.67 to 2.79 g/cc with an average value of 2.726 g/cc. The core analysis revealed also that the upper 30 ft contain hydrocarbon saturation ranged from 0 to 56.5 % with an average value of 15.8%.

In Hil – A9A well, two core plugs were analyzed in this well. The upper plug was located at the top of basement interval, and is about 7 ft thick. Air permeability ranged from 0.007 to 0.65 md with an average value of 0.18 md. The helium porosity ranged from .0.05 to 0.114 with an average value of 0.085. The grain density ranged from 2.62 to 274 with an average value of 2.68. The oil saturation ranged from 5.5 to 20.4% with an average value of 12.3%. The lower core plug, with no logging data, is located at the end drilled basement interval, in which about 39 ft thick were cored in the basement rocks. The core analysis indicated that the air permeability ranged from 0.013 to 69.2 md with an average value of 6.3 md. Helium porosity ranged from 0.018 to 0.115 with an average value of 0.055. Grain density ranged from 2.55 to 2.82 g/cc with an average value of 2.65 g/cc. The oil saturation ranged from 0 to 73.5% with an average value of 27.7%.

Before using the logs, the following steps were carried out:
- The logs are first depth matched
- The logs and core are depth matched
- The logs are digitized
- The raw logs are then environmentally corrected
- Data presentation and statistics results were carried out using IP software program.

3. Geologic setting

The Gulf of Suez is the northern tip of the Red Sea [16]. It is about 300 km long, while the red Sea is about 2000 km long. The Gulf of Suez stratigraphy ranges in age from Precambrian to Recent. This long geologic history of sedimentation was influenced by several factors, such as tectonism and sea level changes, in particular the Suez rifting during the late Oligocene-Miocene and probably through the Pliocene and Recent, which left their marks on the sediments.

Due to the rifting, the stratigraphic succession in the Gulf of Suez was divided into pre-rift, syn-rift, and post-rift sequences (Fig. 2). In this context, the pre-rift sequences represent the strata deposited prior the rift which are separated from the overlying synrift strata by unconformity. The synrift sequences represent the sediments deposited during the extension phase of the rift. The post-rift sequences represent the sediments deposited on the post-rift unconformity. There is a continuous debate about the boundary between the synrift and the post-rift. Should this boundary be placed between the formational units Kareem and Belayim Formations? The last formation marks the waning of the siliciclastic sediments and predominance of evaporites. Other views place the boundary between the Belayim Formation and the overlying salts of South Gharib Formation. In other words, it is placed with the almost domination of evaporites. Either view place the post-rift with the halting of the extension and the high subsidence of the Gulf of Suez.

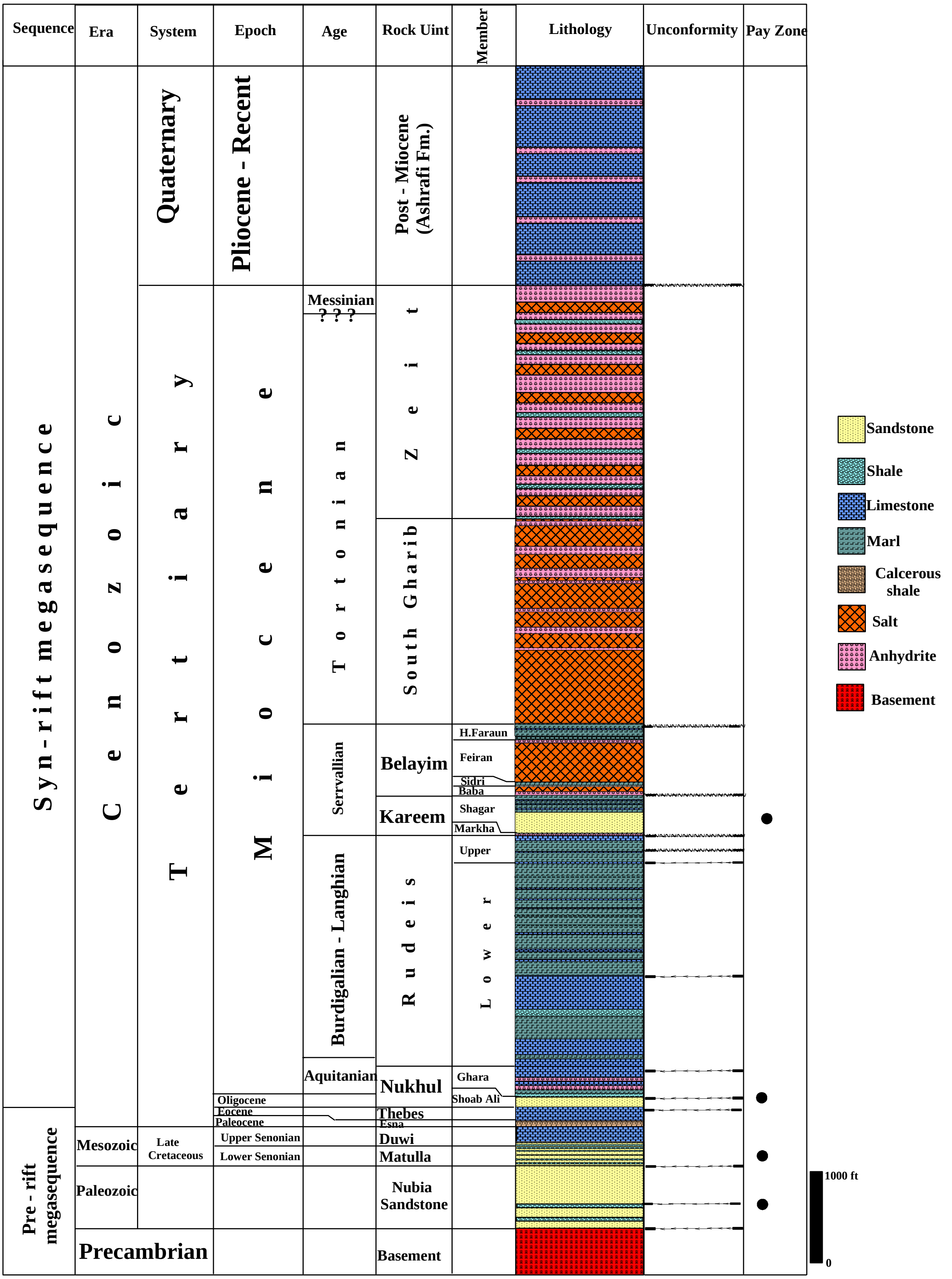

Fig. (2): Generalized stratigraphic column for the central trough of the southern Gulf of Suez

That is implying the evaporites deposition of both South Gharib and Zeit formations was under shallow conditions with presumption of restriction and separation of the Mediterranean and the Red Seas. Under such scenario, Elgamal et al. [17] argued against such presumption and introduced the concept of the Tethys Miocene Salt event. According to this concept, Tethys Miocene evaporites deposition was taking place under active changing in the plate boundaries. Therefore, they considered the evaporites deposition in the Gulf of Suez as a synrift event during which the shoulders of the rift were going under intense uplifting to allow the thick evaporites deposition. The synrift nature of the evaporites and younger Pliocene-Recent sediments would exclude the post-rift aspects. The inclusion of the South Gharib and Zeit formations as well as the younger units in the synrift sedimentation process has been expressed by many authors.

A complex variety of Precambrian metamorphic and crystalline rocks, which dominated by NW and NS, included foliations, fractures, faults, and dikes and cropped out on both Gulf of Suez sides form the basement of the Gulf of Suez. The crust was formed during the widespread pan – African tectono – thermal event. It was developed through the progressive cratonization and accretion of numerous intraoceanic island arcs and Andean – type magmatic arcs during the interval of 780-580 Ma [18]. This event marks formation of the Arabian – Nubian shield. Lithological and structural properties of basement played various roles in rifting [19-21], in which basement rocks influenced the quality and volume of clastic material delivered to the Neogene basin, the Clysmic and Duwi trends are inherited from basement structural discontinuities, basement fabric controls on the location of the accommodation zones, the segmentation of coastal faults and the zig -zag pattern of the tilt – fault blocks.

According to Stern et al. [22], the abundance of east to northeast trending dikes and bimodal volcanic indicates that the crust activity extended and stretched during at least the period 600 –575 Ma. The reactivation of pre-existing discontinuities and their orientation control the evolution of the main fault orientation distribution through time, the geometry of the relay fault zones and the location of fault-controlled basins and depocenters [23]. According to Patton et al. [24], basement rocks formed thoughout two phases; orogenic and anorogenic. The anorogenic phase began with a period of regional NW – SE extension. This extensional period imparts strong fracture strength anisotropy to the basement, which becomes important in deformation during the Mesozoic and tertiary. In general, the basement rocks can be divided into competent granitic intrusions surrounded by less competent zones of metamorphic rocks with intense, NW striking foliations [21].

Generally, the Gulf of Suez tectono – sedimentary evolution passed through the following stages [25]:
- Cambrian - Lower Cretaceous Nubia sandstone stage (continental to alluvial deposits).
- Upper Cretaceous - Eocene stage (open to shallow marine).
- Oligocene - Lower Miocene stage (initial rift stage)
- Horst and graben stage (Lower Miocene)
- Quiescence stage (Middle Miocene)
- Evaporites stage (Middle – Upper Miocene)
- Pliocene – Recent stage.

4. Well logs response to the naturally fractured reservoir:
Well logs can be utilized effectively in identifying the naturally fracture reservoirs. More details can be found in [2, 26-28]. In the following, a brief summary for the response of the well logs to the fractures:

Caliper: formation of mud cake opposite a fracture.
Correction density: high $\Delta\rho$ curve when the hole in gauge.
Natural gamma ray spectroscopy: high uranium content
Density: decrease density
Neutron: increase neutron.
Sonic log: cycle skipping and used to calculate SPI (secondary porosity index)
Induction resistivity: usually not response
Laterolog resistivity: separation between shallow and deep.
Microspherically focused log (MSFL): low reading.
Pe curve: effective only when mud contains barite. In this condition, Pe gives abnormal high
Cluster dipmeter: fractures appear as zones when it has not been possible to make correlation or as dips which seem spurious (abnormal high)
Fracture identification log (FIL): separation of the two pairs of curves
Variable density log (VDL): sudden changes – vague or blurred zones, chevron patterns.
Sonic amplitude: reduction of wave amplitude
According to Schlumberger [26], the best tools to detect fractures are temperature, VDL, MSFL and dipmeter FIL.

RESULTS AND DISCUSSION

Eight drilled bore holes were selected to study the response of different logging tools to the fracture in basement rocks. All the wells are located on structures high. Along the B-Trend, the structure high is capped by salt diapirs, while along the Ghara Trend; the structure high is usually capped by salt pillows (Figs 3&4). The studied wells reached basement at different depths (Fig. 5). The shallowest one was encountered in the southern end of the B – Trend at C-1X well, in which basement encountered at -5985 ft TVDss. The deepest one was encountered in 392-2 well, northern Hilal field (Fig. 6).

SB374-2C well is produced hydrocarbon from Matulla, Nubia sandstone and washed basement [15]. SB374-2C well is located at the northern part of the study area along the prolific B- Trend. The SB 374 field structure is represented by NNW – SSE faulted block on top Nubia, dipping SW dissected by cross fault trending ENE. Hydrocarbon column of more than 1000 ft thick is overlain the washed basement. More than 250 ft thick of basement were drilled in this well (Fig. 7). The response of well logs indicates two obvious facies. Upper facies, from 11070 to 11218 ft depth, is characterized by high interval transit time (ΔT) with an average value of 71 usec/ft. This facies is characterized also by high neutron and low density. However, the most distinctive feature that indicates presence of fracture is the FIL curves response where shadows of the pair of resistivity curves indicate fracture. The lower facies is characterized by low interval transit time with an average value of 52.7 usec/ft, with high density and low neutron. The FIL log indicates no fracture. We can note the response of $\Delta\rho$ in both facies which supporting fractured rocks of upper facies. Gamma ray and SP can't be considered as indicators for fractured basement in this well. There is no obvious separation between ILD and ILM induction log. The net pay is 111 ft thick with an average porosity and water saturation values of 0.138 and 0.12 respectively.

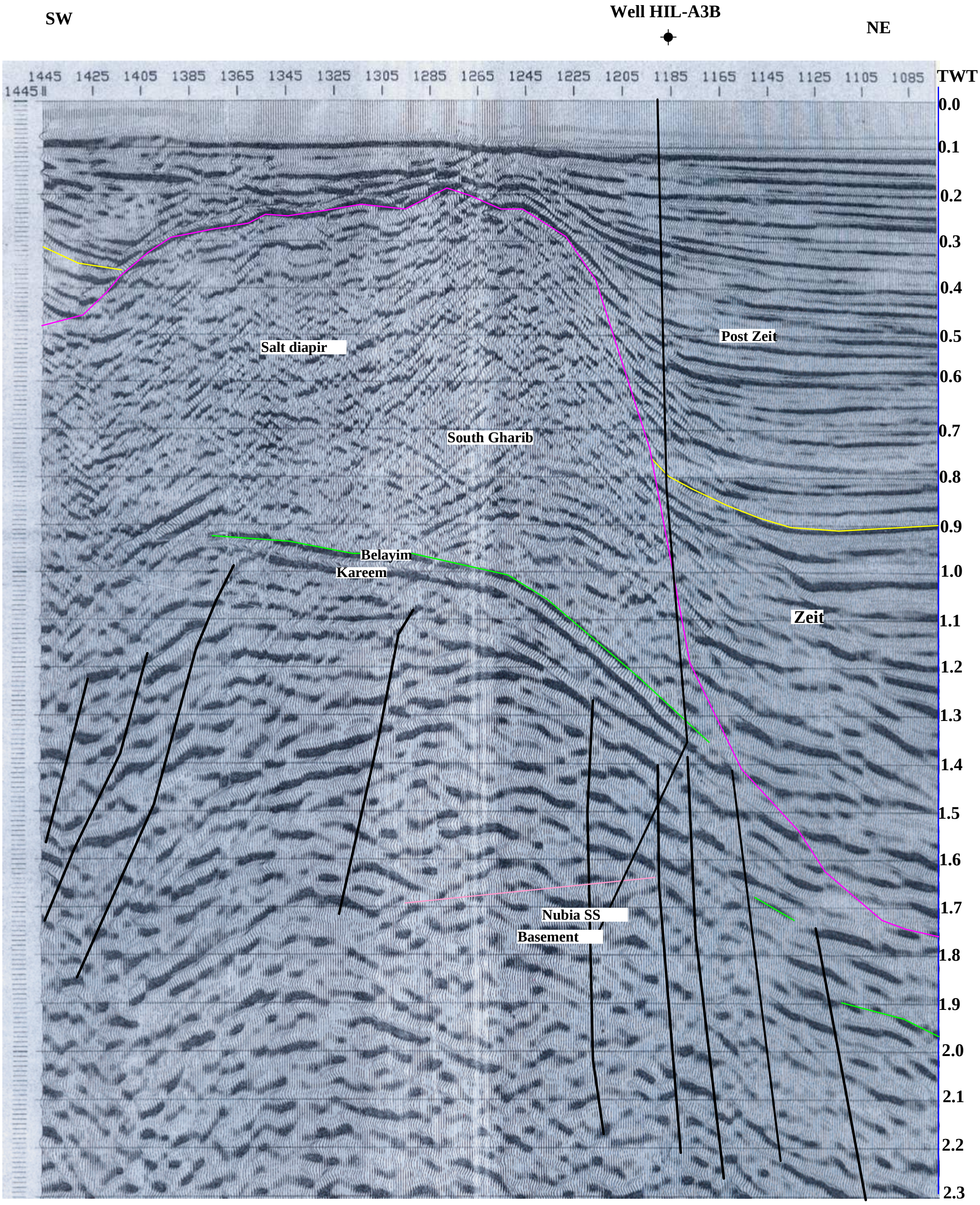

Fig. (3): Seismic line GOS87 -214 interpretation showing high structure in Hilal field. For location refers to Fig. 1

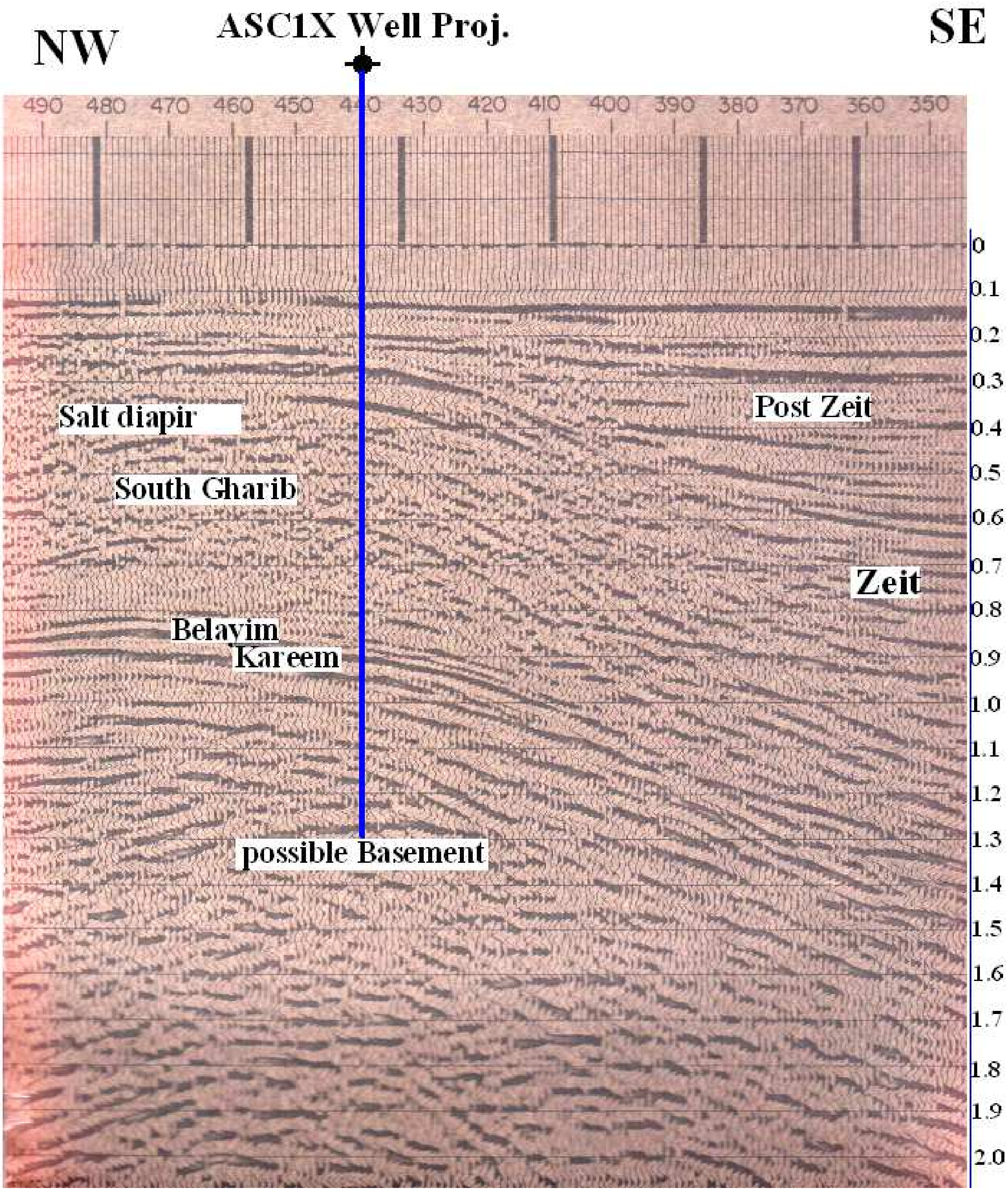

Fig. (4): Seismic line H-41 interpretation showing high structure in Ashrafi field. For location refers to Fig. 1

AS 404- C1X well is located at the southern end of the study area. The well is situated on horst structure (Fig. 4). It represents the shallowest encountered basement amongst the studied wells (Fig. 5). The basement is overlain by the Nukhul clastics. Both Nukhul clastics and basement are produced oil. According to EGPC [15], the Nukhul clastics produced oil at rate 5800 BOPD and basement at rate 2000 BOPD. Beside the core description, which indicates presence of fracture containing hydrocarbon, fractures can be detected from LLS & LLD separation, positive values of Δρ curve when the hole in gauge, uranium content and formation of mud cake (Fig. 8). The separation between LLD and LLS is in the best condition amongst the studied wells. According to Aguilera [2], the larger the separation between LLD and LLS, the wider of fracture opening. In this context, two benefits can be extracted from LLD –LLS relationship; i.e. plotting of LLD/LLS versus LLD and the fracture plausibility as indicated from log (R_{LLD}/R_{LLS}). Rasmus [29] introduced the previous mentioned plot to discriminate between fractured, unfractured and hydrocarbon – bearing fracture zones (Fig. 9). The figure indicated that most of the basement interval is fractured with tendency to bearing hydrocarbon. The threshold value, according to Aguilera [2], for the above logarithmic expression is 0.05, indicating the minimum value of facture plausibility. This corresponds to a resistivity ratio equal to 1.12. A median plausibility is 0.10 indicating a resistivity value equal to 1.26 and corresponding to the half of the fracture plausibility. A maximum plausibility is 0.4 corresponding to a resistivity ratio equal to 2.51. According to this approach, most of the basement interval in C1X well is a median plausibility. Some points are unfractured rocks locating mostly at the lower part and other points are threshold plausibility and occurred at the upper part. Plotting of uranium versus thorium indicates the same results with shift most of the plotted points toward fractured area (Fig. 10). From this plot, basement rocks in his well composed mainly of granite and granodiorite.

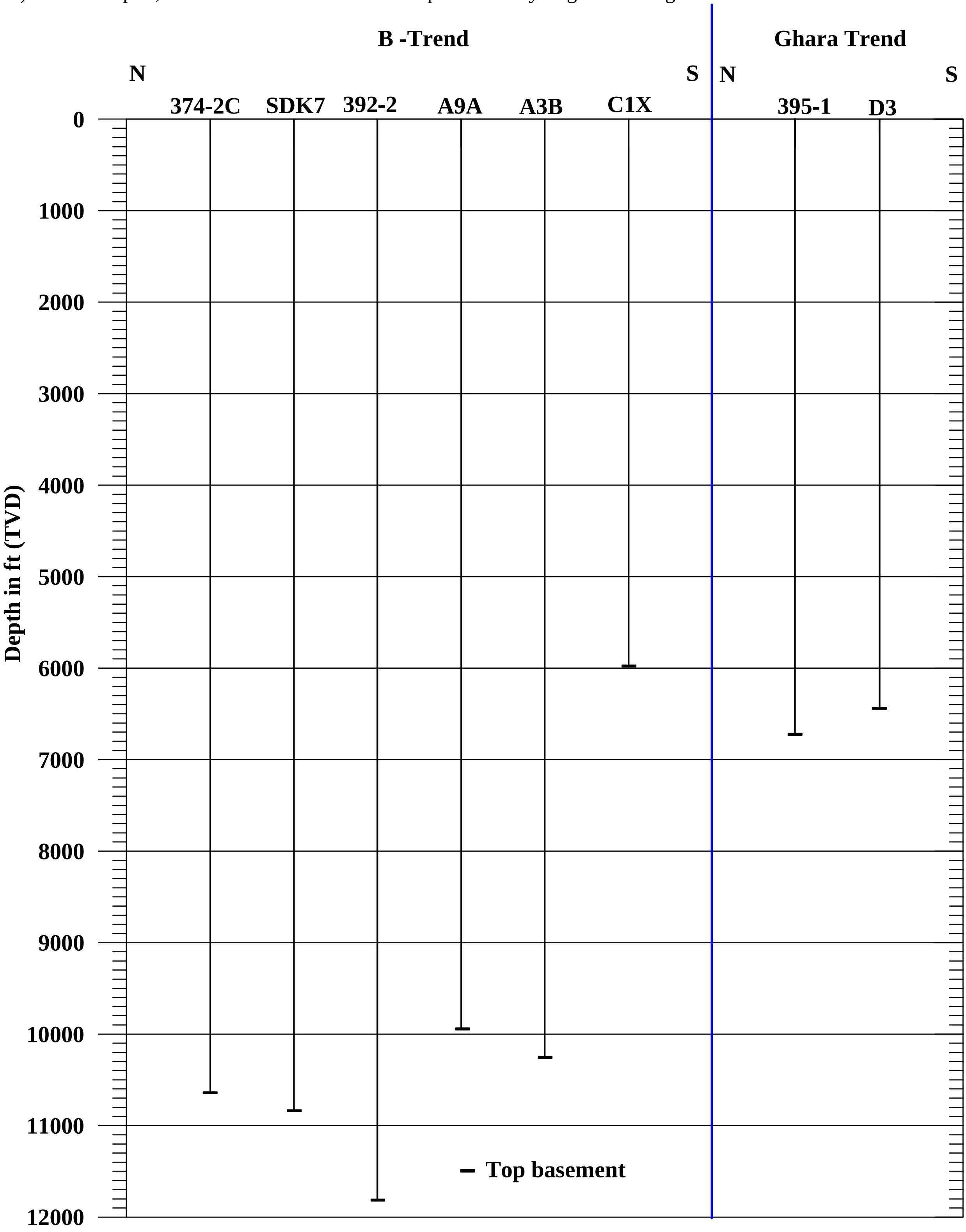

Fig. (5): Depth of top basement in studied wells illustrated shallow depth for Ghara Trend and deep depth for B – Trend

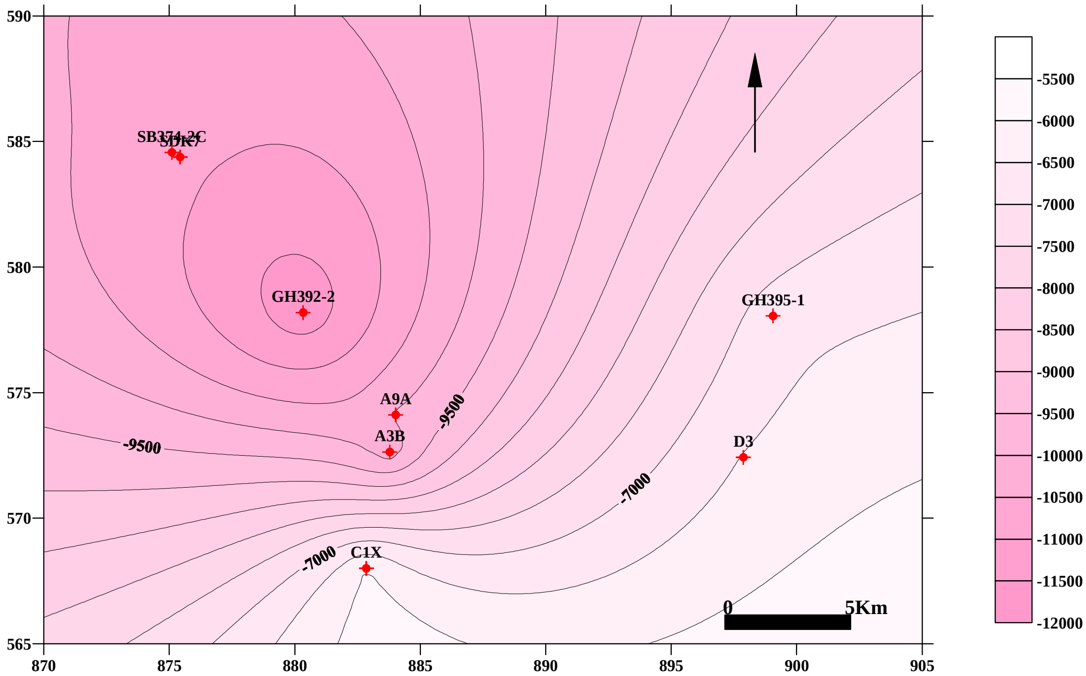

Fig. (6): Depth contour map of the top basement in the southern Gulf of Suez in 2D and 3D

SDK7 well is located in the northern part of the study area along the B –Trend. The basement is overlain by about 700 ft of hydrocarbon productive Nubia sandstone. This well provides a good opportunity to correlate between fractured and unfractured rocks in the same interval. Fractures can be detected from FIL log which indicates about 35 ft thick of fractured basement at the top of the basement interval (Fig. 11). Neutron can be used to confirm presence of fractures. Uranium versus thorium indicates a weathered zone located at the top of the basement interval (Fig. 10). This plot indicates that basement rocks composed mainly of granodiorite. The uranium concentration in the fractured zone is the same as in C1X well (average value of about 7 ppm) (Table 1). While in the unfractured interval, the average U concentration decreased to 2.2 ppm. However, density log can't be differentiating between fractured and unfractured rocks. Sonic log indicates decreasing interval transit time from above 60 to about 52 usec/ft in the unfractured interval. The most important feature can be observed in this well is the response of induction resistivity log in both fractured and unfractured rocks. In the former, Rt ranges from 1 to 10 ohm.m. In the later, resistivity responses similar to the anhydrite rock with 2000 ohm.m. This means that, in basement rock, it is so easy to differentiate between fractured and unfractured rocks using resistivity logs.

A3B well is located in the southern part of the study area on a horst structure (Fig. 3). The well is produced oil from the Nubia sandstone which unconfromably underlain by basement rock. This well provides a good chance to study the response of FIL and cluster dipmeter processing, VDL and sonic amplitude to the fractured rocks. Other conventional well logs are available (Fig. 12). Neutron log indicates increasing porosity at the upper part. Density, Pe and sonic logs cannot assess in detecting fracture in this well. Dipmeter of cluster processing indicates two sets of trends. However, dipmeter of FIL processing, VDL and sonic amplitude put our hands on the locations of the fractures. The fractured zones appear on VDL as a wavy pattern. This wavy pattern of the interval as well as low resistivity (maximum value of 174 ohm.m) argued for fractured basement for the entire interval (Fig.12).

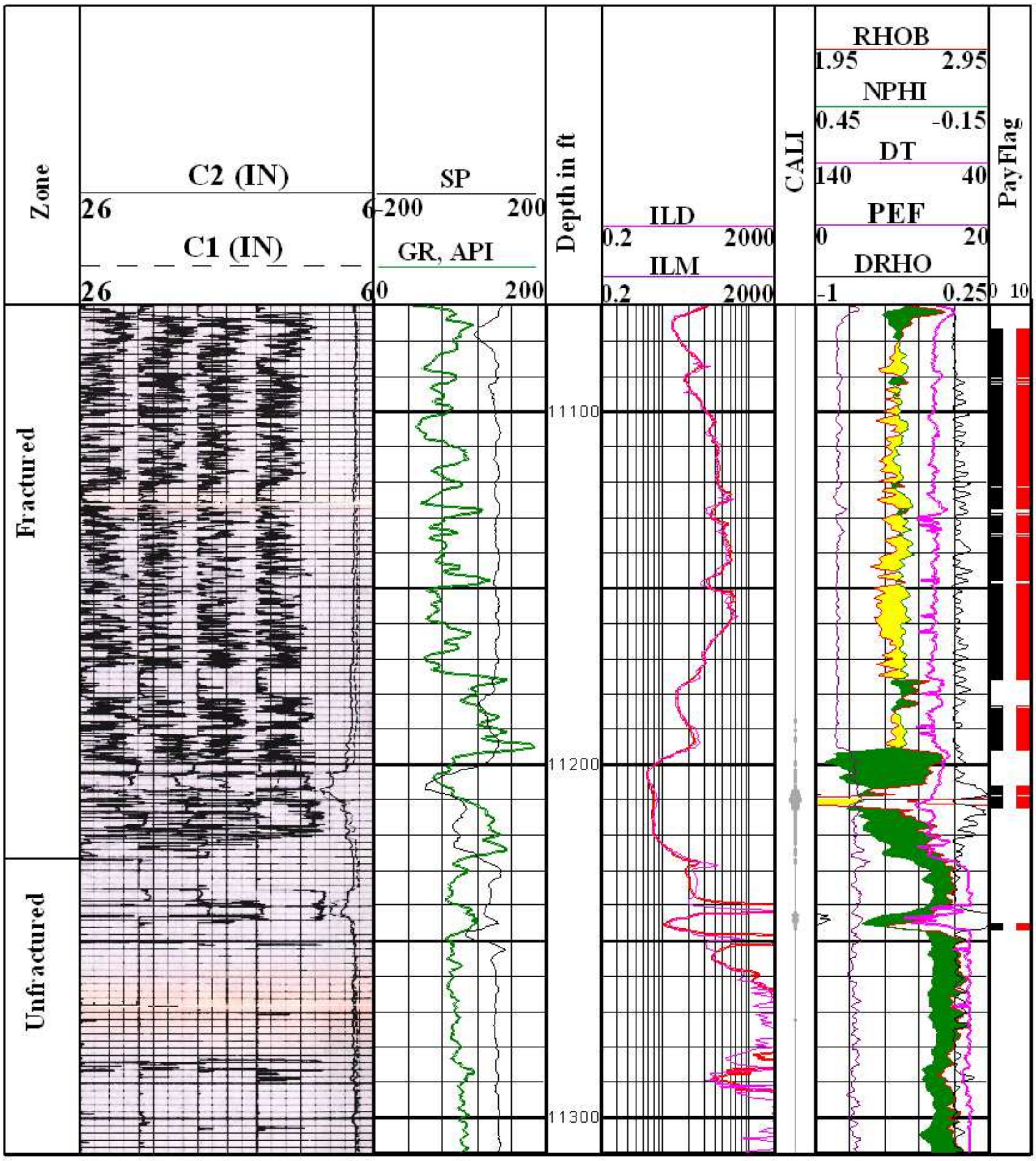

Fig. (7): Two zones can be detected in SB374-2C well. Fractured zone at the upper part with low Pe, high ΔT, high NPHI, and low RHOB as well as +ve DRHO. Unfactured zone, lower interval, with high Pe, low ΔT, low NPHI, high RHOB and very high resistivity

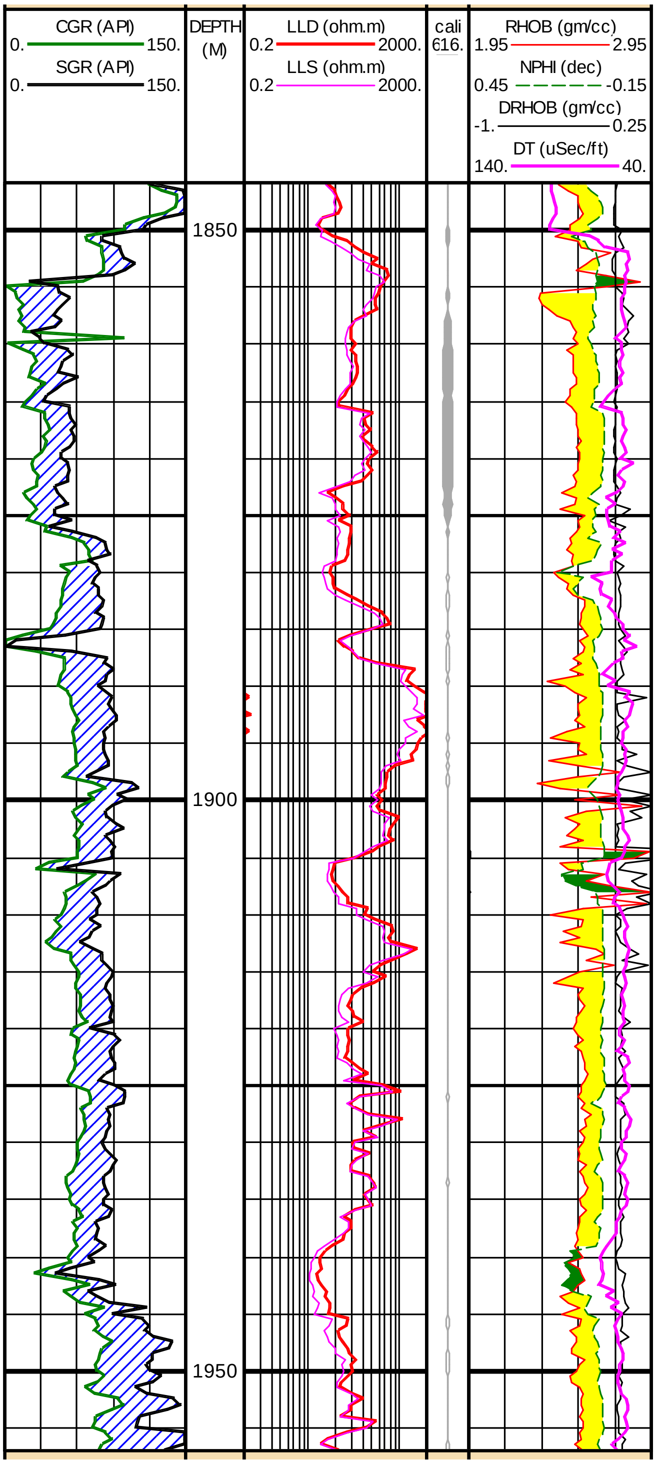

Fig. (8): Basement rock interval in AS404-C1X well. The entire interval is fractured as indicated from LLD – LLS separation, +ve DRHO, and high uranium concentration

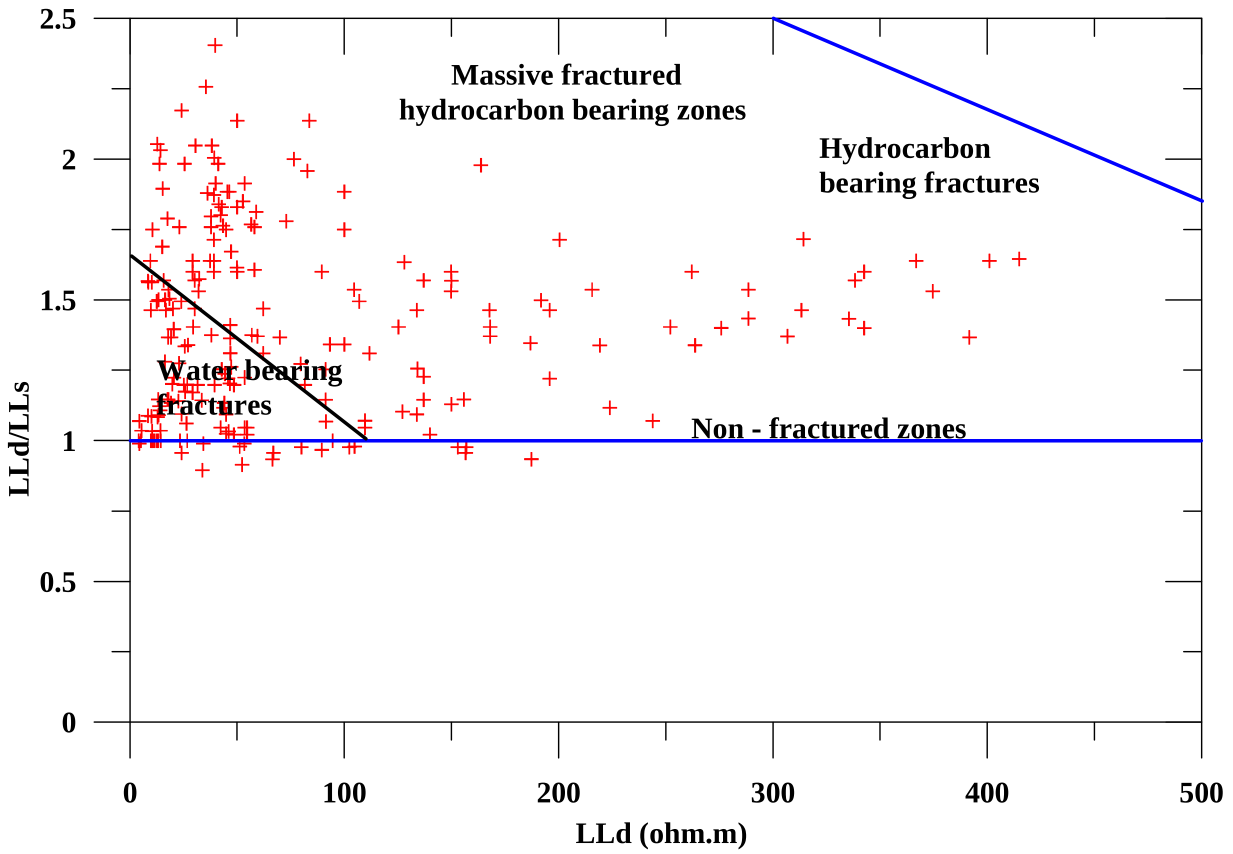

Fig. (9): Plotting of LLD/LLS versus LLD differentiated between fractured and unfractured zones in AS404-C-1X well. Hydrocarbon bearing zones can be identified from this crossplot

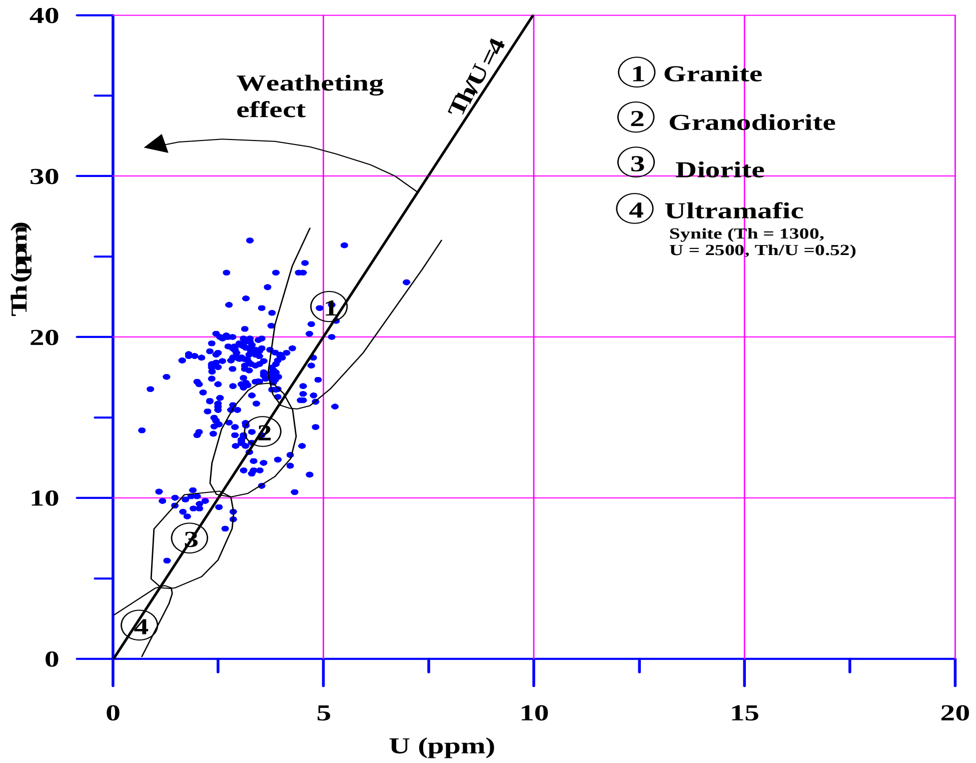

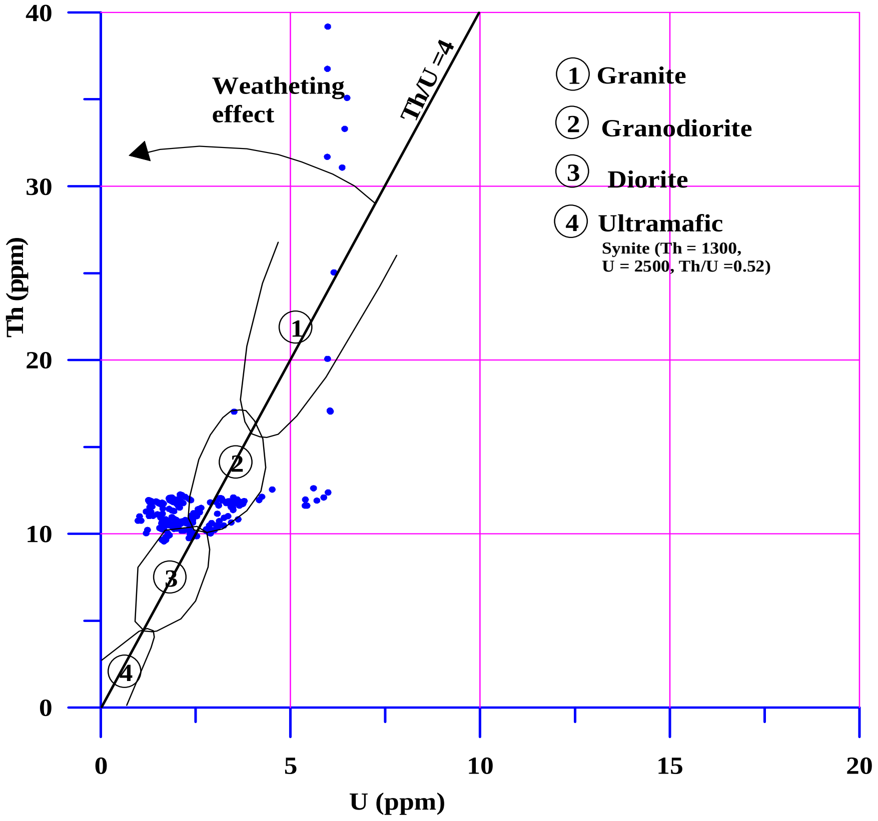

Fig. (10): Plotting of Thorium versus uranium contents in both AS404-C1X and SDK7 wells illustrated type of igneous rocks as well as identified the weathering effect [30]

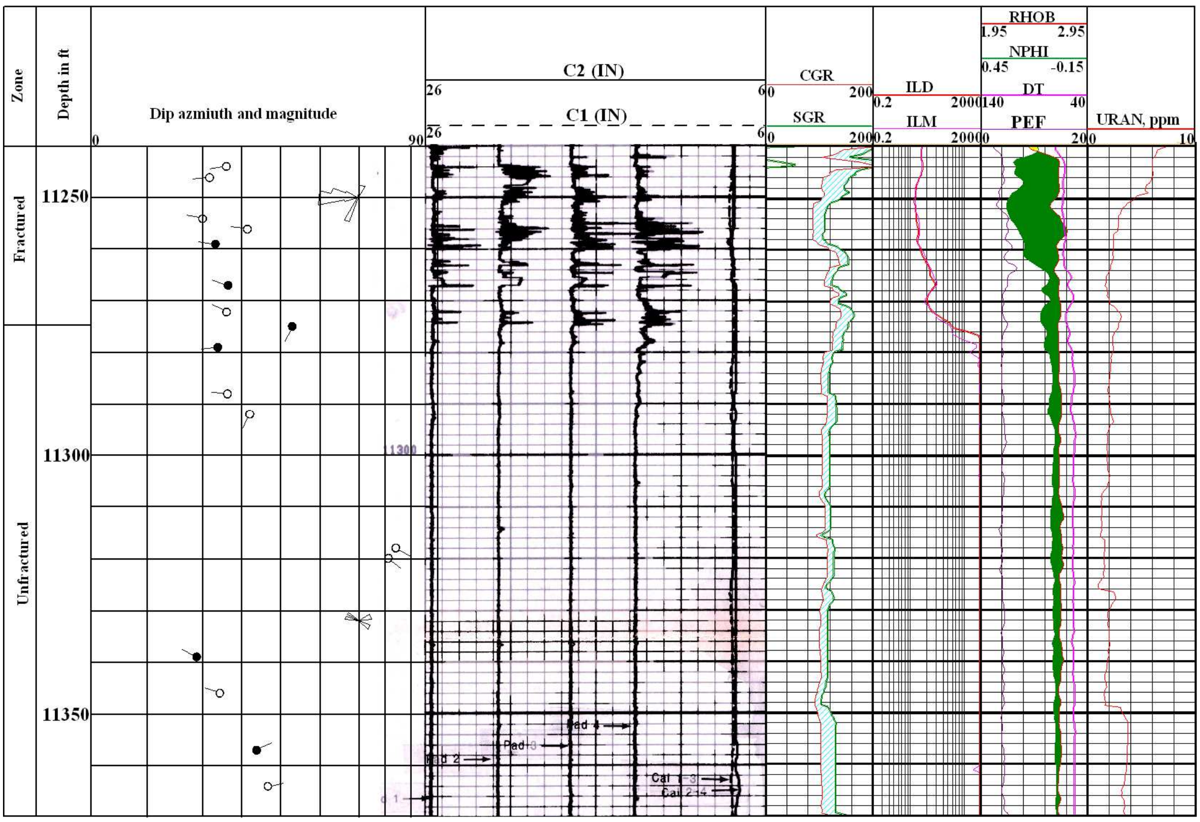

Fig. (11): Basement interval in SK7 well. Two zones can be identified. Upper zone, fractured rocks, with high NPHI, high U, low ILD and shadows in FIL log. The lower zone, unfractured one, with two distinctive features associated with this interval; high ILD (2000 ohm.m) and no shadow in FIL log

Table (1): Statistics of well logs response to the fractured and unfractured basement

well		parameter	GR	RHOB	NPHI	DT	PE	URAN	THOR	POTA
AS404-C1X		Min	2	2.32	0.001	48		7	6.1	1
		Max	149	2.95	0.161	95		0.7	26	5.9
		Avg.	80	2.55	0.03	58.5		3.1	16.9	4.3
SDK7	. Frac.	Min	259	2.4	0.057	52.8	2.37	1.6	9.5	0.5
		Max	107	2.76	0.305	69.8	6.9	7.2	39.2	5
		Avg.	147	2.67	0.182	60.4	4.5	3.4	13.2	3.3
	Unfrac	Min	154	2.7	0.022	51.8	3.5	1	10	3.5
		Max	104	2.72	0.072	55.3	5.2	3.8	17	4.3
		Avg.	123	2.7	0.041	52.5	4.2	2.2	11.3	3.7
GH395-1		Min	591	2.02	0.004	50.6				
		Max	52	2.79	0.488	110				
		Avg.	124	2.5	0.113	61.9				
GS392-2		Min	100	2.55	0.057	51				
		Max	55	2.77	0.18	58				
		Avg.	81.5	2.66	0.112	55				
SB374-2C	Frac.	Min	187	2.16	0.107	59.7	2.1			
		Max	54	2.7	0.417	83	5.3			
		Avg.	93	2.41	0.179	70.8	2.9			
	unfrac.	Min	155	2.36	0.023	49	3.6			
		Max	84	2.85	0.29	89	6.2			
		Avg.	103	2.72	0.075	54.5	4.5			
Hil-A9A		Min	150	2.4	0.016	56.9				
		Max	62	2.73	0.254	88.5				
		Avg.	110	2.61	0.124	67				
Hil-A3B		Min	307	2.39	0.06	51.8	2.3			
		Max	71	2.68	0.46	75	5.6			
		Avg.	112	2.6	0.201	60.4	4.1			

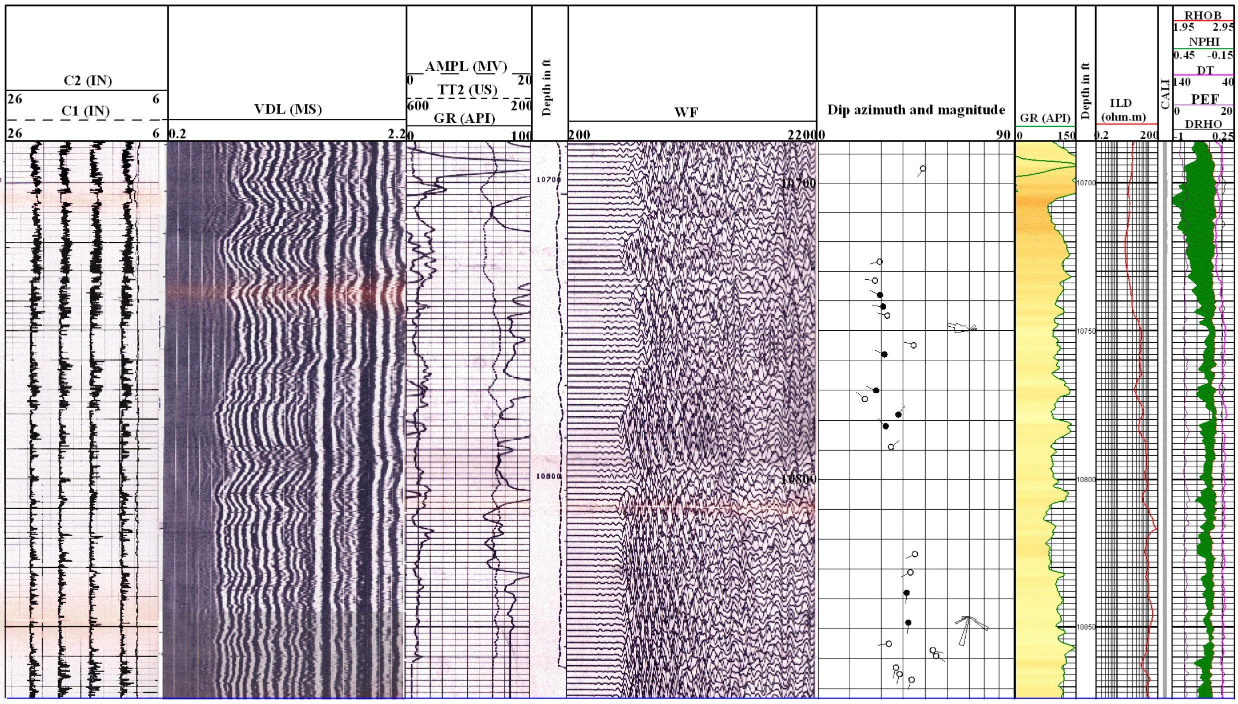

Fig. (12): Integration between conventional logs and VDL, FIL and sonic amplitude illustrated the response to fractures in Hil-A3B well

In GS392-2 well, basement is overlain unconfromably by the Nukhul Formation, in which Nubia sandstone and Upper Cretaceous sequence is faulted out. No oil production was recorded in this well. However, the gas composition analysis indicates that the hydrocarbon composition is as the following: C1 = 14400, C2 = 1500, C3= 600 and traces for C4. As noted, C1/C2 ratio equals to 9.6 and C1/C3 ratio = 24; meaning that the zone is oil – bearing, according to Aguilera [2]. Neutron log records increasing porosity and density correction curve gives high positive values indicating fracture rocks (Fig. 13). In this well, laterolog resistivity (LLD and LLS) and microspherical focused log (MSFL) provide the identification tools of fracture. Resistivity logs are the main provider for fracture information. The separation between LLD and LLS as well as low reading of MSFL indicates fracture of the entire interval. Plotting of LLD/LLS versus LLD indicates wholly fractured interval (Fig. 14). However, dipmeter of FIL processing indicates unfractured interval. This means that the fracture system may be horizontal rather than vertical, in which FIL log cannot detect it. Mineral solver using IP program indicates possible pay zone at the lower part of the logged interval corresponding to the widest separation between LLD and LLS.

GH395-1 well is located along the Ghara Trend toward the eastern margin of the Gulf of Suez. The basement rock is overlain unconformably by the Nubia sandstone. No hydrocarbon production is recorded in this well. About 350 ft thick was drilled in this well. Integration between density, neutron, density correction curve, dipmeter (abnormal high in cluster processing) and resistivity indicates fractured basement for the entire interval (Fig. 15). However, plotting of LLD/LLS versus LLS indicates considerable points located behind the unfractured line (Fig. 16). This may be attributed to using of fresh mud filtrate, in which in water – bearing formation, LLS reads equal or higher than LLD.

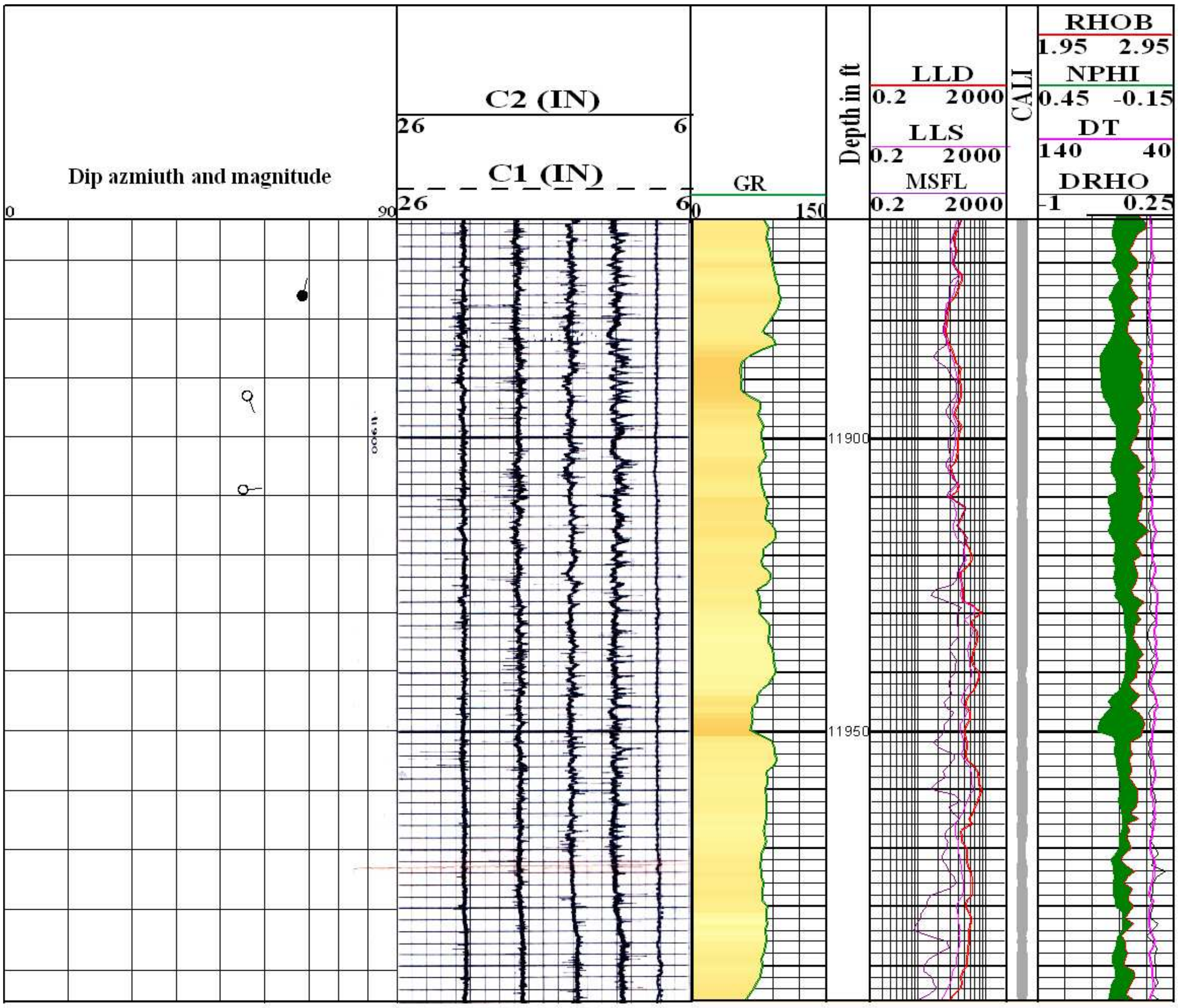

Fig. (13): Fractured basement in GS392-2 well can be detected from low MSFL, LLD –LLS separation, high NPHI, low RHOB, high dip magnitude. However, FIL log indicates unfractured interval. This may be attributed to the fracture systems are horizontal rather than vertical

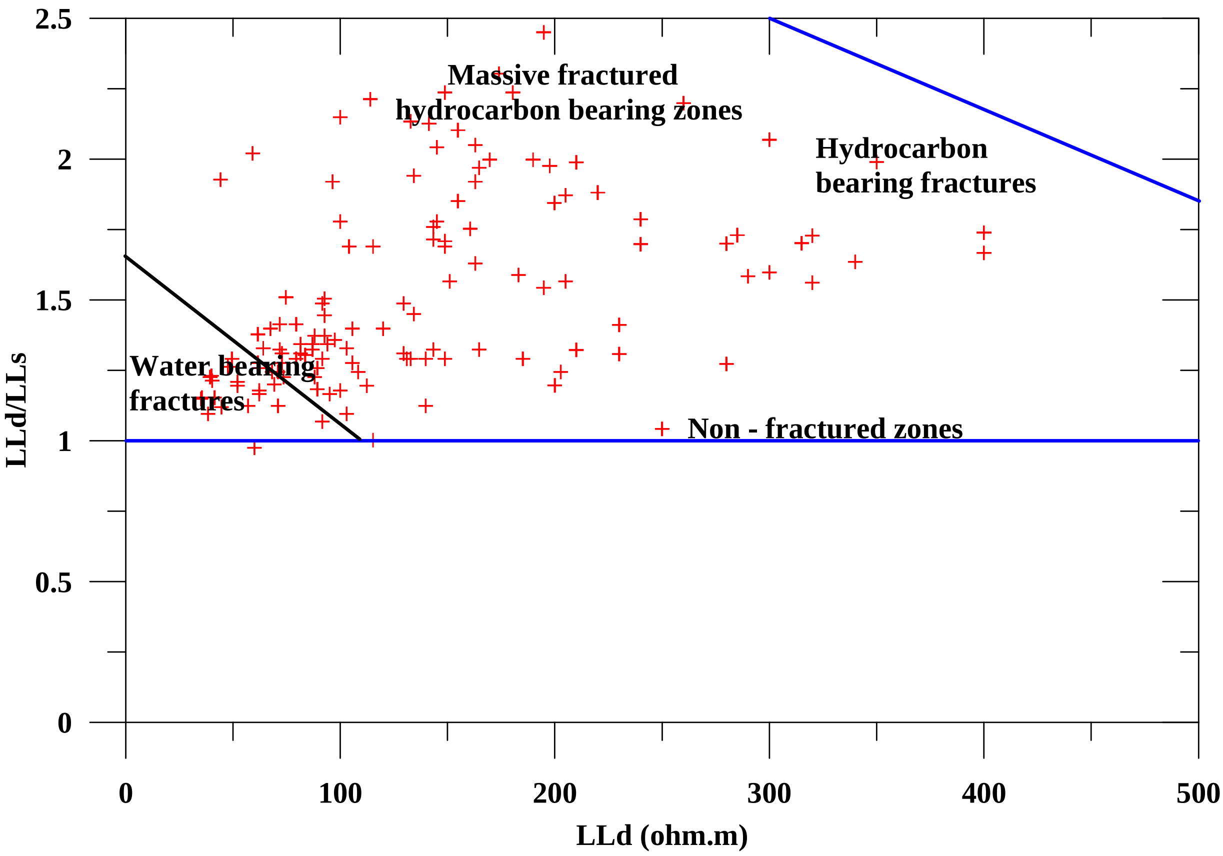

Fig. (14): Plotting of LLD/LLS versus LLD differentiated between fractured and unfractured zones in GS392-2 well

CONCLUSION

Basement rocks in the southern Gulf of Suez composed mainly of granite and granodiorite. In all studied wells, the upper part of the encountered basement is usually fractured. The thickness of fractured interval is varied from one well to another. Usually, the produced wells from fractured basement are overlain by a hydrocarbon column from which they are sourced. Qualitative identification of the fractured basement can be carried out using the conventional geophysical logging tools. In basement, it is easy to differentiate between fractured and unfractured using resistivity logs either laterolog or induction. In unfractured basement, the resistivity response is similar to its response to anhydrite (very high resistivity = 2000 ohm.m.). In fractured basement, resistivity gives variable readings according to the fluid – filled pores. Neutron, density and sonic logs as well as density correction curve are responses to fractures but their responses must be supported by other tools such as FIL processing dipmeter, which can be considered as one of the most effective tools in identifying fractures.

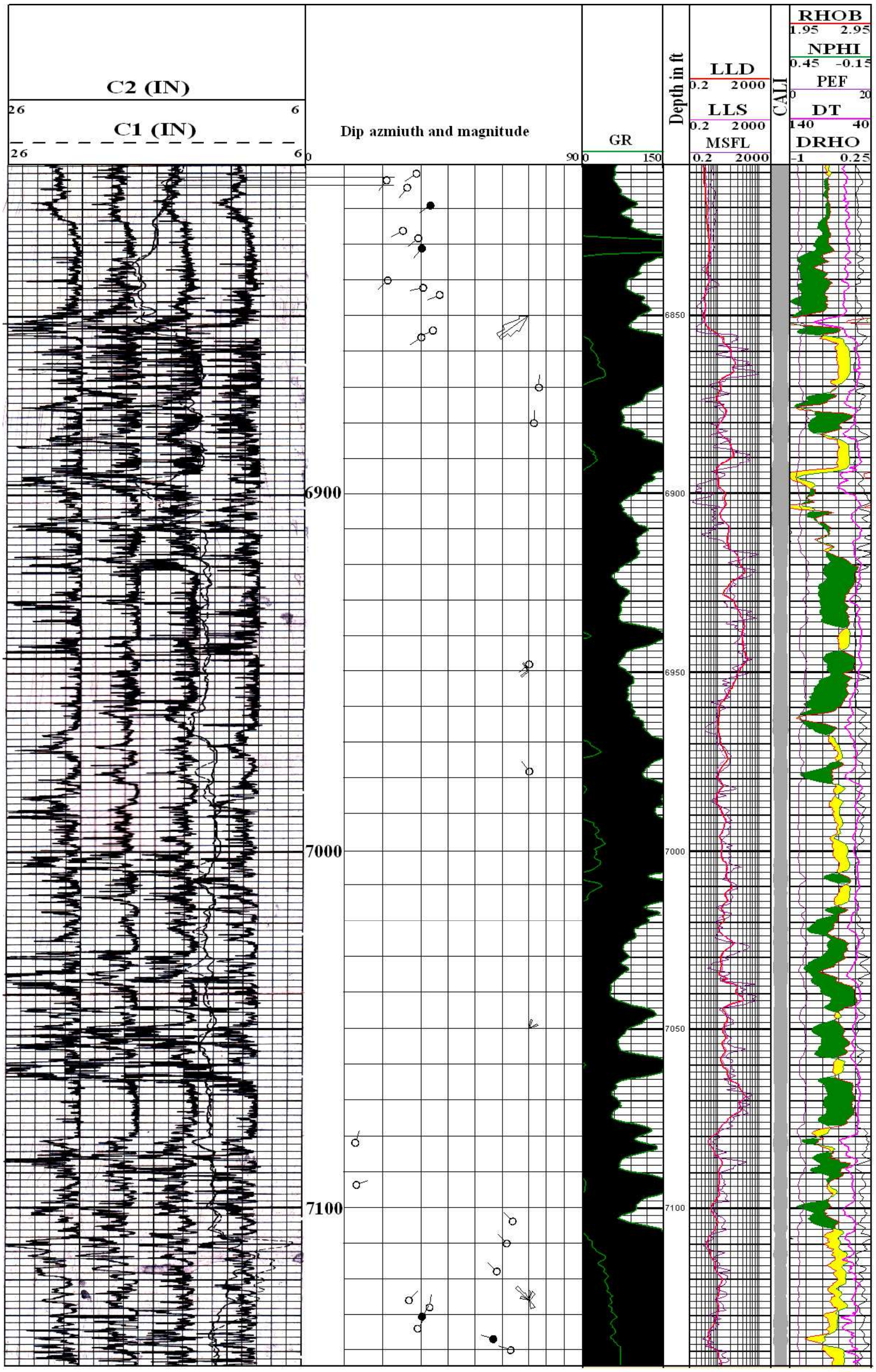

Fig. (15): The drilled basement interval in GH395-1 well. All the available logs argued for presence of fractured rocks. Abnormal high dip magnitude is obvious throughout the entire interval

Acknowledgements

The Author is grateful to the Egyptian General Petroleum Corporation (EGPC) and the Gulf of Suez Petroleum Company (GUPCO) for providing the data.

REFERENCES

[1] R. A. Nelson; Geologic Analysis of Naturally Fractured Reservoirs, Gulf Publishing Co. Book Division, **2001**.
[2] R. Aguilera; Naturally Fractured Reservoirs, 2nd ed., PennWell Books, Tulsa, Oklahoma, **1995**.
[3] S.M. Luthi, In: P.K. Harvey, T.S. Brewer, P.A. Pezard, and V.A. Petrov, (eds), Petrophysical Properties of Crystalline Rocks (Geological Society, London, Special Publication 240, **2005**) 95.
[4] M. G. Salah, A. S. Alsharhan, *Journal of Petroleum Science and Engineering*, **1998**, 19, 201.
[5] A. Sircar, *Current Science*, **2004**, 87, 147.
[6] J.C. Gutmanis, *IPTC*, **2009**, 13156.
[7] M. Lefranc, , S. Farag, L. Souche, A. Dubois, AAPG International Conference and Exhibition, Singapore, September 16-19, **2012**.
[8] S.D. Gupta, R. Chatterjee, M.Y. Farooqui, *J. Geophys. Eng*., **2012**, 9,162.
[9] M. Suardana, , A. Samodra, A. Wahidin, M.R. Sule, AAPG Annual Convention and Exhibition, Pittsburgh, Pennsylvania, May 19-22, **2013**.
[10] K.K. Landes, J.J. Amdruso, L.J. Charlsworth, E. Heany, P.J. Lesperance, *American Association of Petroleum Geology Bulletin*, **1960**, 44, 1682.
[11] S.M. Selim, K.M. Abdallah, AAPG Annual Convention and Exhibition, Long Beach, California, April 22- 25, **2012**.
[12] I. Zahran, S. Askary, 9th EGPC Petroleum Exploration and Production Conference, Cairo, **1988**, 1, 163.
[13] F. El Wazeer, F. Ismail, 9th EGPC Petroleum Exploration and Production Conference, Cairo, **1988,** 1, 68.
[14] F. Ismail, I. El Moula, Proc. 12th EGPC Explor. Semin. Cairo, **1994**, 1, 206.
[15] Egyptian General Petroleum Corporation, EGPC; Gulf of Suez oil fields (A comprehensive overview), **1996**.
[16] I. Moretti, J. Gargani, AAPG Annual Convention, San Antonio, Texas, April 20-23, **2012.**
[17] M.M. Elgamal, H. El Araby, M.S. Aly, 5th International Conference on the Geology of the Arab World, Feb., **2000**.
[18] A.E.J. Engel, T.H. Dixon, R.J. Stern, *Geological Society of America Bulletin*, **1980,** 91, 699.
[19] C. Montenat, P. Ott d'Estevou, and B. Purser, In: C. Montenat (ed.), Geological studies of the Gulf of Suez, northwestern Red Sea coasts, tectonic and sedimentary evolution of Neogene rift: Documents et Travaux Institut Geologique Albert de Lapparent, 10, **1986,** 7.
[20] A. I. Younes, K. McClay, 14th EGPC Exploration and Production Conference, **1998**, 1, 35.
[21] A.I. Younes, K. McClay, *AAPG Bulletin*, **2002**, 86, 1003.
[22] R.J. Stern, D. Gottfried, C.E. Hedge, *Geology*, **1984**, 12, 168.
[23] N. Bellahsen, J.M. Daniel, *Journal of Structural Geology*, **2005**, 27, 769.
[24] T.L. Patton, A.R. Moustafa, R.A. Nelson, A.S. Abdine, In: S.M. Landon (ed.), Interior rift basins: AAPG Memoir, **1994**, 59, 9.
[25] M.A. Omran, M.S. El Sharawy, *Arabian Journal of Geosciences*, **2014**, 7, 87.
[26] Schlumberger; Well Evaluation Conference of Algeria, **1979**.
[27] Schlumberger; Well Evaluation Conference, Egypt, Services Techniques Schlumberger, France, **1984**.
[28] Schlumberger; Log Interpretation Principles/Applications, , Sugar Land, Texas, **1989.**
[29] J.C. Rasmus, JPT, **1982**, 2673.
[30] O. Serra; Fundamentals of Well –Log Interpretation. 1 – the acquisition of logging data, **1984**, Elsevier Science Publishers B.V.